Analysis on the Effectiveness of the 20-H Rule for Printed-Circuit-Board Layout to Reduce Edge-Radiated Coupling

Mark I. Montrose, *Senior Member, IEEE*, Er-Ping Li, *Senior Member, IEEE*, Hong-Fang Jin, and Wei-Liang Yuan, *Member, IEEE*

***Abstract*—This paper presents the quantified study of the electromagnetic radiation mechanism of the 20-H rule using a numerical approach that has not yet been systematically addressed. The 20-H rule is a rule-of-thumb layout technique recommended to minimize radiated fields propagating from the edges of a printed circuit board (PCB) coupling onto nearby structures. Propagating electromagnetic fields may corrupt adjacent cable assemblies, sheet metal enclosures, and aperture openings. The magnitude of this design rule is investigated using the full-wave finite-difference time-domain (FDTD) method. An analysis on whether benefits exist from use of this rule is examined and under what conditions the rule is valid when correctly implemented. The purpose of this paper is to provide insight into the validity of the 20-H rule, recognizing that every PCB will have different simulation results. FDTD is used to capture a snapshot view of field propagation. This view allows one to determine the validity of the 20-H rule at a single point of time within a dynamic structure and what may be expected when digital components are finally added to a PCB assembly, which generally negates simulated results.**

***Index Terms*—Finite-difference time-domain (FDTD) simulation, printed circuit board (PCB), 20-H rule.**

I. Introduction

THE 20-H RULE states that the physical size of a power plane in a high-density *multilayer* stackup topology must be physically smaller than its corresponding return plane by a dimension equal to 20 times the distance separation between the two planes. The application of this rule of thumb and when it is or is not appropriate has not been well defined due to the complexity of the design concept, theory involved, and understanding how to setup a proper model that truly describes operation of the rule. For historical reasons, the 20-H rule was discovered and first implemented nearly 25 years ago to solve specific problems observed with printed-circuit-board (PCB) design and layout.[1] This design technique, which was proprietary for years but has been implemented by many companies since then, was first released into the public domain in 1996 [1].

Manuscript received May 19, 2003; revised September 22, 2004.

M. I. Montrose is with Montrose Compliance Services, Inc., Santa Clara, CA 95051-1214 USA (e-mail: m.montrose@ieee.org).

E.-P. Li, H.-F. Jin, and W.-L. Yuan are with the Institute of High Performance Computing and the National University of Singapore, Singapore 117528 (e-mail: eplee@ihpc.a-star.edu.sg; engp1063@nus.edu.sg; yuanwl@ihpc.a-star.edu.sg).

Digital Object Identifier 10.1109/TEMC.2005.847383

[1]The concept of the 20-H rule was first modeled and implemented by W. Michael King, who also coined the term *20-H rule*, circa 1980.

The 20-H rule provides termination of propagating electromagnetic fields from digital components that switch large amounts of peak power current during cross conduction. By itself, the 20-H rule may be appropriate to implement with actual (resistive/capacitive) components.

Undercutting a plane to the physical location of digital components provides the same level of benefit to terminating propagating fields rather than adding discrete components, which is an alternate layout technique that adds cost to an assembly. In many cases, components may not terminate planes efficiently [2].

Power and return planes must be treated as if they are an actual digital signal transmission line. A propagating electromagnetic wave will return to its source after encountering a high-impedance load or termination, which in this case, is the physical edge of the PCB. A signal integrity situation exists except this time it involves propagating fields within the dielectric separating the power and return plane, similar to a signal transmission line with a source driver and its corresponding return path. This condition assumes the edge of the planes extend significantly beyond the physical location of the components that are connected to the planes [3].

Until now, there has been no quantified radiation mechanism study on the 20-H rule. Designers have misinterpreted the need for this rule with assumptions as to how and why the rule works. This paper investigates, using multiple configurations and frequencies, the magnitude of board-edge RF radiation present, providing knowledge to PCB and electrical designers as to whether the 20-H rule is fact or fiction.

Section II describes test configurations. Section III provides the simulation model, with results in Section IV. Sections V and VI present Poynting vector calculations.

II. Test Configuration

To investigate the 20-H rule accurately, extensive computing power is required. Attempts to analyze the 20-H rule have been made with conflicting analysis using only one physical dimension or configuration [4]. Other research validates claims made herein [5].

The uniqueness of this paper takes into account the following:

1) *Evaluation at different frequencies*: determines if plane resonances affect performance and if the rule is valid across the frequency spectrum or only at nonresonant frequencies of the PCB plane pair.

2) *Evaluation at different planar spacing*: different distance spacing between power and return planes examines at what separation distance the 20-H rule becomes valid.
3) *Evaluation with different board configurations*: multiple configurations: 0-H, 5-H, 10-H, 15-H and 20-H along with different board dimensions assess if a resonance condition exists and the magnitude of benefit for this design rule.

Due to the nature of the problem definition, as well as calculating the total magnitude of the propagating electromagnetic field that resulted from simulation, attempting to correlate simulated data with actual measurements from a test PCB in an anechoic chamber would *not* provide benefit for correlation purposes due to the following reasons:

1) measurement uncertainty of the test environment and instrumentation exceeds power levels present;
2) the problem is a *near-field* effect and measurement in an anechoic chamber generally is intended to occur in the *far-field*;
3) the extremely low-level RF power present cannot be easily measured with any degree of accuracy;
4) a test board with a stimulus connection (SMA connector) would probably radiate more RF energy due to the installation of the connector than the actual fields that propagate from the edge of the PCB.

In a typical PCB assembly, near-field flux can cause possible coupling of undesired RF energy to adjacent metallic structures and cable assemblies. Due to the extremely low levels of radiated power present, it is difficult, if not impossible, to measure the exact magnitude of a propagating field on an operational PCB with hundreds of components changing logic states along with I/O cables attached to the assembly.

In a real PCB, the calculated propagating field from finite-difference time-domain (FDTD) simulation will always be *magnitudes less* than fields generated by operational circuits or that provided by a stimulus source using a standard SMA connector (which itself by installation could radiate a field).

Measurement uncertainty of most instrumentation is typically $+/-3$ dB, which is significantly greater than the magnitude of the propagating field present between the power and return plane pair. This is why attempting to measure the magnitude of edge radiated emissions in an anechoic chamber is difficult, if not impossible on a fully populated PCB, or even using a test stimulus source yet benefits may be observed during testing and certification on a final, operational product using this design rule.

III. System Model Implementation

In order to simulate the 20-H rule accurately, a three-dimensional (3-D) model was developed that took into consideration the electromagnetic field present at the same point in time and space. Fig. 1 illustrates the basic model used.

The following assumptions are made.

1) Both the power and return plane are perfectly conducting and satisfy these conditions in the positions of the two planes.

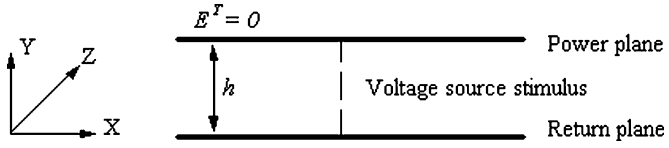

Fig. 1. Dimensional source model (uniform voltage configuration).

2) Both planes are infinitely thin in thickness (compared to width and length).
3) Simulation is based on free space.
4) The source stimulus is located at a distance that is centered equally between the two planes.

Free space was truncated into finite rectangles in which the edges of each rectangle include reasonable perfectly match layers (PMLs). These PMLs are then used for the absorbing boundary condition (ABC) for this FDTD model.

Three types of stimulation sources were available for simulation: Gaussian, dipole, and uniform voltage. All three sources were investigated in the early stages of this research project and produced similar, if not identical results. For reporting purposes in Section IV, the uniform voltage source stimulus was chosen.

The uniform voltage source used the formulation $E_{\text{line}} = E_0 \sin(2\pi fkdt)$. According to definition, this stimulus is described by

$$V = \int Edy = E_0 \sin(2\pi fkdt) * h = V_0 \sin(2\pi fkdt) \quad (1)$$

where f is the frequency of the source, k is the time step number after discretization of Maxwell's equations, h is the distance spacing between planes, and dt is defined by the function $dt = \Delta x/2c_o$ where c_o is the speed of light.

IV. Simulation Results

During the process of validating results from simulation, 3-D analysis was first performed using an enhanced and proprietary version of FDTD software named MAFIA. The same configuration was reanalyzed using standard two-dimensional (2-D) FDTD. The distribution of the $\boldsymbol{E}$ field in the z axis was investigated for accuracy. The difference between the 2-D and 3-D model was within 1.7%. For this reason, the 2-D simulator was deemed accurate enough for this analysis.

Our first set of 2-D simulation provides the electromagnetic field distribution for both $\boldsymbol{E}$ and $\boldsymbol{H}$ fields separately. The following three test configurations are examined, each at three different frequencies to determine if undercutting the power plane to other than 20-H causes different results. The separation distance between planes is $h = 0.25$ mm (10 mils). The physical length of the power plane is 2 cm (0.78 in).

1) 0-H at 300 MHz, 600 MHz, 900 MHz.
2) 10-H at 300 MHz, 600 MHz, 900 MHz.
3) 20-H at 300 MHz, 600 MHz, 900 MHz.

The physical length of the power plane at 2 cm was chosen to represent a PCB dimension commonly found in high-density assemblies, e.g., typical physical component placement relative

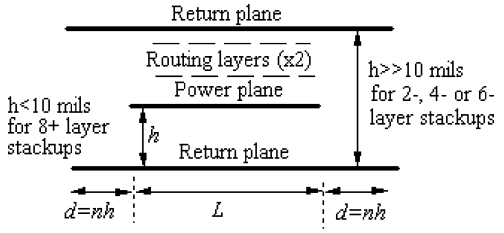

Fig. 2. Planar structure model for all simulation configurations.

to the edge of the PCB. In addition, the three frequencies chosen are also generally found on many PCB designs.

The purpose of the 20-H rule is to provide board edge termination of propagating waves, similar in concept to signal integrity for digital circuits (transmission-line theory). Power and return planes must be analyzed as transmission lines. For example, if a digital component is located at the end of a signal transmission line that is not properly terminated, any length of that transmission line which travels past the end of the component becomes a stub antenna. It is this stub antenna that drives the planes as a dipole antenna. Few high-density PCBs have components located *greater* than 2 cm from the edge of the board. This research simulates a typical PCB, not one based on a theoretical dimension commonly used for academic analysis such as 10 cm.

The test PCB is modeled as a planar structure (Fig. 2). Separation distance between the two planes is "h." This distance is chosen to represent an actual *multilayer* PCB assembly. Instead of making the power plane smaller, the return plane is extended by n (0, 5, 10, 15, 20). The 20-H rule performs best when used within an eight or more layer high-density PCB assembly, *not* a two-, four- or six-layer stackup where the distance spacing between plane pairs is generally greater than 0.25 mm (10 mils).

With regard to Fig. 2, one may try to simulate this planar model with a return plane located equidistant above the power plane, thus making the power plane a true stripline configuration. In a real PCB with eight or more layers, the physical layers that would be located directly above the power plane would be two signal layers, *not* another plane (either power or return potential). The physical distance between the power plane and its associated reference plane (Fig. 2) would be significantly greater in distance separation than 0.25 mm (10 mils).

Figs. 3 and 4 illustrate the field amplitude radiating from the edge of this model at popular frequencies. These plots illustrate field distribution in the immediate vicinity of the PCB (near-field coupling) at a single point of time but do not offer information regarding the total magnitude of board-edge radiation that can cause potential harm. This element of research is investigated in Sections V and VI.

For Figs. 3 and 4, the uniform voltage source was used as the stimulus (Section III). Fig. 3 shows the electric field ($\boldsymbol{E}_x$) at 300, 600, and 900 MHz with different distances of the extended return plane. Fig. 4 is identical to Fig. 3 except that the magnetic field ($\boldsymbol{H}_z$) is shown. For all plots, the physical size of the power plane was constant; only the return plane was extended.

The primary area of concern lies not with the flux pattern but with the effects that the flux has on adjacent circuits, metallic enclosure, card guides, or cable assemblies that can and will couple this propagated energy by capacitive means. It is the total *magnitude* or steady-state condition of the radiated energy we should be concerned with and *not* the flux pattern that we view in the time domain.

Analysis of Fig. 3 indicates that, for the electric field, significant benefit occurs at 900 MHz. At 300 MHz, benefit is also achieved; however, at 600 MHz, there appears to be minimal improvement.

In Fig. 4, the magnetic field component is investigated. We again achieve significant benefit at 900 MHz with improvement at 300 and 600 MHz. It appears that, if the extended return plane was increased to a distance greater than 20-H, any flux that remains should be captured by the return plane, thus validating the 20-H rule as fact.

It is to be noted that FDTD provides only a snapshot view of field propagation at *one* specific point of time. RF field propagation, both $\boldsymbol{E}$ and $\boldsymbol{H}$ will be different for all dynamic configurations examined at any other time period. Although transient results differ as time moves on, steady-state propagating fields generally do not change. Steady-state analysis for all configurations is presented in Sections V and VI.

Why then is dynamic analysis performed? Results from FDTD allow one to visualize field propagation after steady-state conditions have been met. The plots of Figs. 3 and 4 are a snapshot view that illustrates clearly that the 20-H rule is valid under certain configurations and frequencies and not others. Sometimes, a brief visualization of a single point of time (Figs. 3 and 4) provides "insight" into a sophisticated layout rule of thumb prior to examining the steady-state condition.

V. Poynting Vector Calculation

We now calculate the magnitude of the propagating electromagnetic field off of the edge of the board. The Poynting vector is chosen for this calculation

$$P = \boldsymbol{E} \times \boldsymbol{H} (\mathrm{w/m^2}) \tag{2}$$

where $\boldsymbol{E}$ and $\boldsymbol{H}$ are denoted as electric and magnetic field strengths, respectively.

Since $\boldsymbol{E}$ and $\boldsymbol{H}$ are both instantaneous field vectors, the interpretation that $\oint_s E \times H \cdot ds$ is equal to the power flowing out of a closed surface applies in this simulation.

As a simplified example on how to calculate the Poynting vector, the emitted energy from a 2-D structure is the integration of the power density along edges AB, BC, CD, and DA, as shown in Fig. 5.

When calculating the Poynting vector, 3-D simulation was performed based on the simplified 2-D concept of Fig. 5, whereas, in Section IV, 2-D plots are provided showing field density, not the magnitude of radiated energy density.

With regard to discretization, the following integral equation is used:

$$\oint_{\mathrm{ABCD}} P \cdot dl = -\int_{\mathrm{DA}} P_x dl + \int_{\mathrm{BC}} P_x dl. \tag{3}$$

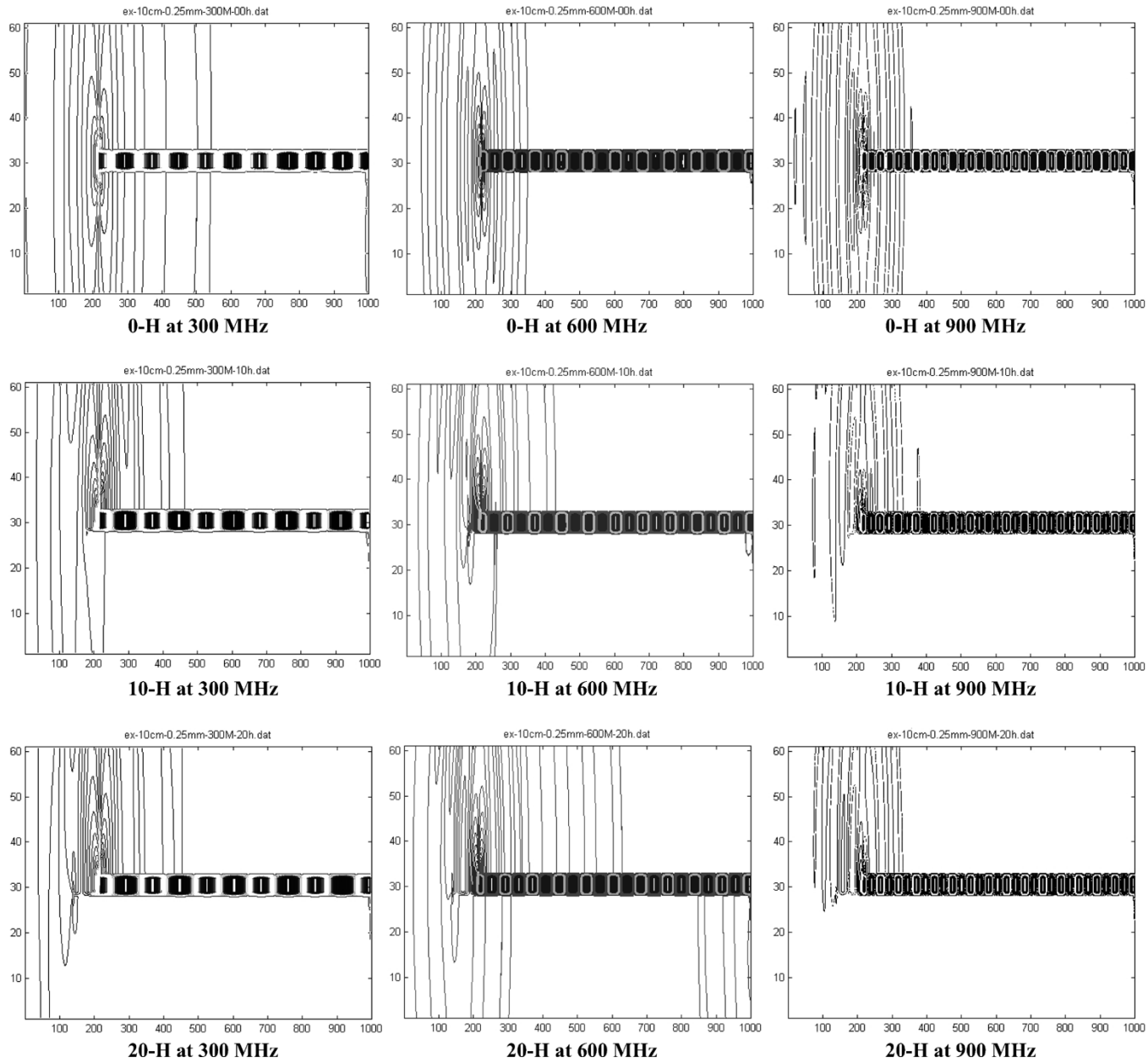

Fig. 3. Electric field distribution map ($\boldsymbol{E}_x$): frequency versus the x-H rule (h =0.25 mm or 0.01 in).

For the TE mode, the field component $E_x = 0$, therefore $P_y = 0$. Similarly, for the TM mode, we have $E_y = 0$. This permits $P_x = 0$. Since the magnetic flux is perpendicular to the y axis, when the source is parallel to the y axis, we observe only the Tm_y mode [4].

Because of the symmetry of the structure, integration along the closed line can be simplified as the integration of line BC by

$$\oint_{\mathrm{ABCD}} P \cdot dl = 2 \int_{\mathrm{BC}} P_x dl. \tag{4}$$

When studying electromagnetic field propagation, it is not obvious how propagating waves travel. For convenience of understanding field propagation, we calculate the Poynting vector (both $\boldsymbol{E}$ and $\boldsymbol{H}$ field wave propagation) based on the results of Figs. 3 and 4. Using Fourier transformation and Matlab, we are able to create the tables in Section VI.

VI. Poynting Vector Results

A. Effects of Distance Separation Between Planes

A dipole sinusoidal excitation source is applied to both planes. The branches of the dipole are equal to the physical length of the respective power and return planes. Different from the uniform voltage excitation, the dipole source will not change with separation distance. This property provides convenience when different separation distances are studied. The excitation source is described by (5).

$$E = 10\,000 \sin(2\pi f k dt) \text{ V/m} \tag{5}$$

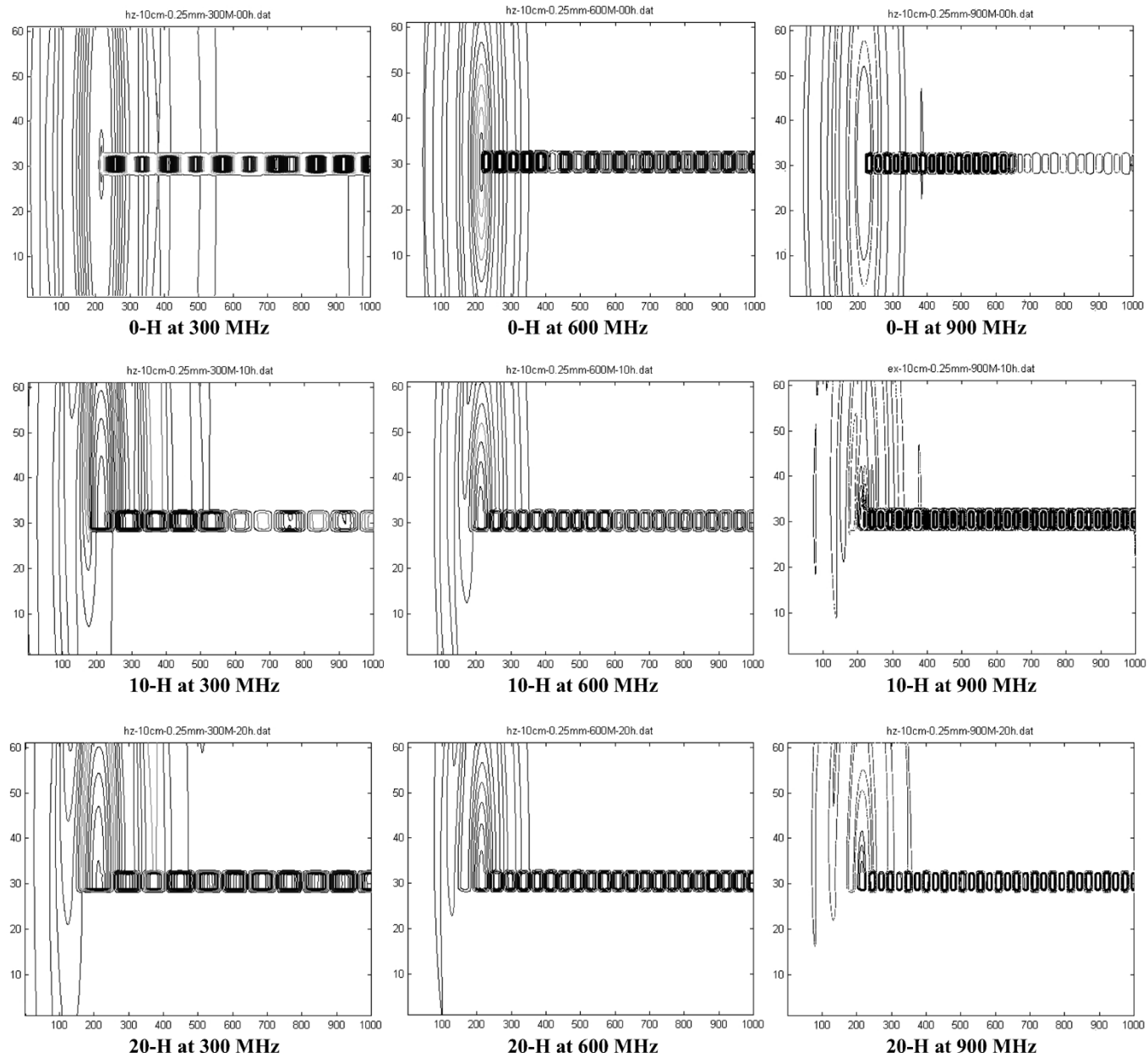

Fig. 4. Magnetic field distribution map ($\boldsymbol{H}_z$): frequency versus the x-H rule (h =0.25 mm or 0.01 in).

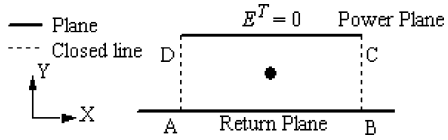

Fig. 5. Sample configuration for calculation of the Poynting vector.

TABLE I
RADIATED POWER VERSIS SEPARATION DISTANCE (POWER PLANE LENGTH $L = 2$ cm, $h = 0.6$ mm [24 mils], $f = 600$ MHz)

Distance of extended reference plane to create	Edge radiated power (nanowatts)
0-h	86.51
10-h	8.41
20-h	4.95

where f is the source frequency, k is the time step in the FDTD algorithm, and $dt = \Delta t = 1.667 \times 10^{-13}$ (s).

The frequency 600 MHz appeared to be the only frequency of the three not affected by use of the 20-H rule per Figs. 3 and 4. For this reason, we investigate this particular frequency in greater detail. The physical location where the data is tabulated is at the edge of the return plane.

Tables I–III illustrate the radiated power from the EM field present propagating from the extended PCB edge. The propagated electromagnetic field is given in the form of the integration of $P(t)$.

The physical dimensions of this PCB had the power plane fixed at 2 cm long (0.78 in) with a separation distance h at 0.6, 0.4, and 0.2 mm (24/16/8, mils respectively). The value of 2 cm is a typical physical distance that a component may be located from the edge of the PCB. This component, when switching

TABLE II
RADIATED POWER VERSUS SEPARATION DISTANCE (POWER PLANE LENGTH $L = 2$ cm, $h = 0.4$ mm [16 mils], $f = 600$ MHz)

Distance of extended reference plane to create	Edge radiated power (nanowatts)
0-h	124.67
10-h	11.74
20-h	6.61

TABLE III
RADIATED POWER VERSUS SEPARATION DISTANCE (POWER PLANE LENGTH $L = 2$ cm, $h = 0.2$ mm [8 mils], $f = 600$ MHz)

Distance of extended reference plane to create	Edge radiated power (μwatts)
0-h	186.90
10-h	17.59
20-h	9.53

logic states, provides the stimulus source that drives a transmission line: an unterminated stub. When simulations are performed, perfect stimulus sources are generally provided which may not describe how a fully populated PCB behaves under operational conditions.

The simulated results show that the separation distance between the power and return planes does not alter the effectiveness of the 20-H rule. However, the extended length of the return plane does greatly affect the magnitude of the radiated power off of the edge of the PCB. It may not be necessary to extend the return plane to a distance of 20-H for optimal benefits, i.e., 10-H may be sufficient.

It is therefore not proper for design engineers to assume that a 20-H extension is required for every PCB stackup assignment and for every frequency throughout the spectrum due to internal board resonances.

B. Effects of an Extended Return Plane Versus Frequency

To analyze effects of PCB resonances due to application of the 20-H rule, various configurations of an extended return plane was simulated at different frequencies. A uniform voltage source (6) is now provided as the stimulus instead of the dipole source. Results are listed in Table IV. The resulting field is located at the physical edge of the return plane

$$E = 1000\ \sin(2\pi f k dt)\ \text{V/m} \tag{6}$$

Simulation voltage was 0.6 V. The power plane was recessed at 2 cm with a distance spacing between planes set to $h = 0.4$ mm (16 mils). All other test conditions from Section VI were identical.

For this configuration, extending the return plane significantly minimized board edge radiated effects at 300, 600, and 900 MHz, as detailed in Table IV.

C. Effects of a Physically Larger Size PCB Versus Frequency

The power plane was doubled in physical size from $L = 2$ cm to 4 cm while maintaining distance separation at $h = 0.4$ mm (0.016 in or 16 mils). The reason why we changed the physical size of the PCB was to determine if the self-resonant frequency of the assembly also changes and by how much, along with the effects on application of the 20-H rule related to edge-radiated emissions.

TABLE IV
RADIATED POWER VERSUS. SOURCE FREQUENCY (POWER PLANE LENGTH $L = 2$ cm, $h = 0.4$ mm)

Distance of extended reference plane to create	Edge radiated power (μwatts)		
	300 MHz	600 MHz	900 MHz
0-h	316.30	767.37	705.20
5-h	55.60	135.08	124.71
10-h	31.16	76.34	72.40
15-h	22.02	54.52	53.37
20-h	17.26	43.22	43.74

TABLE V
RADIATED POWER VERSUS LARGER SIZE POWER PLANE (POWER PLANE LENGTH $L = 4$ cm, $h = 0.4$ mm)

Distance of extended reference plane to create	Edge radiated power (μwatts)		
	300 MHz	600 MHz	900 MHz
0-h	1077.16	2404.31	1464.14
5-h	186.83	420.26	266.09
10-h	105.31	241.22	167.45
15-h	74.80	174.57	132.30
20-h	58.78	139.77	120.39

TABLE VI
RADIATED POWER VERSUS LARGER SIZE PCB AND SEPARATION DISTANCE (POWER PLANE LENGTH $L = 6$ cm, $h = 0.6$ mm)

Frequency	Configuration	Edge radiated power (milli-watts)
150 MHz	0-h	1.556
150 MHz	5-h	0.275
600 MHz	0-h	11.481
600 MHz	5-h	2.107
900 MHz	0-h	4.357
900 MHz	5-h	1.082

According to Table V, increasing the physical length of the power plane will increase board-edge-radiated emissions slightly and again at the higher frequencies. It can thus be concluded that changing the physical size of a PCB has minimal effect on the performance of the 20-H rule.

D. Effects of Board Resonance Versus Frequency

When another physical configuration is investigated, we observe that resonances inside the PCB significantly affect the magnitude of the propagating field when an extended return plane is provided. For this round of simulation, both dimension L and frequency f for different structures are analyzed. The results in Table VI show that the physical size of the PCB will affect 20-H rule implementation mainly through resonances

within the PCB. When L is larger, it is easy to create resonances, even when the stimulus is not very high, such as 600 MHz.

VII. Conclusion

The 20-H rule is quantitatively investigated using the numerical approach FDTD with embedded SPICE to include field propagation and transmission-line termination. Depending on the physical size of the PCB and distance spacing between the power and return planes, there are enormous resonances inside the PCB. A PCB will be resonant at typically one primary frequency. This specific frequency will change based on whether the board is bare (theoretical analysis) or contains active digital components (real-world usage).

In a normal configuration, 0-H, both electric and magnetic field distribution is symmetric, both vertically and horizontally. After implementing the 20-H rule, flux distribution will be altered significantly. The results of a shield plane physically located above the power plane would prevent z-axis EMI, thus only x- and y-axis propagating fields should be our primary area of concern when dealing with the 20-H rule.

Three factors, namely operating frequency, separation distance between planes, and physical size of the PCB affect implementation and benefits from use of the 20-H rule. *Regardless of configuration, the 20-H rule is proven to be fact, not fiction*. Simulated results show that the separation distance between the power and return planes does not alter the effectiveness of the 20-H rule. However, the extended length of the return plane does greatly affect the magnitude of the radiated power off of the edge of the PCB. It may not be necessary to extend the return plane to a distance of 20-H for optimal benefits, i.e., 10-H may be sufficient.

The 20-H rule is recommended only for high-density multilayer assemblies with multiple power and return planes. By containing both electric and magnetic fields at the edge of the PCB, can benefit be observed when testing to both FCC and CISPR emission requirements? If improper use of the 20-H rule is implemented, near-field coupling may increase [2].

References

[1] M. Montrose, *Printed Circuit Board Design Techniques for EMC Compliance—A Handbook for Designers*, 2nd ed. New York: Wiley/IEEE Press, 2000.

[2] M. Montrose, E. Liu, and E.-P. Li, "Analysis on the effectiveness of printed circuit board edge termination using discrete components instead of implementing the 20-H rule," in *Proc. IEEE Int. Symp. EMC*, pp. 45–50.

[3] M. Montrose *et al.*, "Analysis on the effectiveness of the 20-H rule using numerical simulation technique," in *Proc. IEEE Int. Symp. EMC*, pp. 328–333.

[4] H. W. Shin and T. Hubing, "20-H rule modeling and measurements," in *Proc. IEEE Int. Symp. EMC*, pp. 939–942.

[5] C. Schuster and W. Fichtner, "Parasitic modes on printed circuit boards and their effects on EMC and signal integrity," *IEEE Trans. Electromagn. Compat.*, vol. 43, no. 4, pp. 416–425, Nov. 2001.

[6] Y. Jiang, *Printed Circuit Board Design Rule Analysis and Simulation by FDTD Method*, Singapore: Nat. Univ. of Singapore, 2001.

[7] A. Taflove, *Computational Electrodynamics: The Finite Difference Time-Domain Method*. Boston, MA: Artech House, 1995.

[8] W. Yuan and E.-P. Li, "FDTD simulation for hybrid circuits with linear and nonlinear lumped elements," *Microw. Opt. Technol. Lett.*, vol. 32, no. 6, pp. 408–412, Mar. 2002.

Mark I. Montrose (S'74–M'79–SM'93) received the B.S. degree in electrical engineering and the B.S. degree in computer science from California Polytechnic State University, San Luis Obispo, both in 1979, and the M.S. degree in engineering management from the University of Santa Clara, Santa Clara, in 1983.

Currently he is owner and principal consultant of Montrose Compliance Services, Inc., Santa Clara, a full-service regulatory compliance company specializing in electromagnetic compatibility (EMC) design and testing, working in the field for 25 years. He has authored four books published by Wiley/IEEE Press dealing with EMC and printed-circuit-board design and layout, and testing for EMC compliance, which includes international translations. In addition, he has published papers within IEEE dealing with advanced concepts of printed circuit board design rules.

Mr. Montrose is a member of the Board of Directors of the IEEE Electromagnetic Compatibility Society (EMCS) and the first President of the IEEE Product Safety Engineering Society. Other activities within IEEE include being a member of the IEEE Press Board. Recognitions within the IEEE EMCS include being a Distinguished Lecturer. He has received numerous citations for his work within the society, including two of the three highest awards given by the society, which are the Technical Achievement Award and the prestigious Laurence G. Cummings Award for outstanding service to the IEEE EMCS over the course of many years.

Er-Ping Li (M'92–SM'01) received the M.Sc. degree from Xi'an Jiaotong University, Xi'an, China, in 1986 and the Ph.D. degree from Sheffield Hallam University, Sheffield, U.K., in 1992, both in electrical engineering.

He worked as a Research Fellow from 1989 to 1990 and then as a Lecturer from 1991 to 1992 at Sheffield Hallam University. Between 1993 and 1999, he was a Senior Research Fellow, Principal Engineer, and Technical Manager/Director with the Singapore Research Institute and Industry. Since 2000, he has been with A-STAR Institute of High Performance Computing, Singapore, where he is currently a Senior Scientist and Senior Research and Development Manager of the Computational Electromagnetics and Electronics Division. He has published over 90 technical papers in international referred journals and conferences and coauthored three book chapters. His research interests include fast and efficient computational electromagnetics, EMC/EMI, signal integrity analysis, and computational nanotechnology.

Dr. Li has served as international conference chair numerous times. He is a Technical Advisor to multinational companies in Asia and is also a Senior Fellow with the National University of Singapore.

Hong-Fang Jin received the B.Sc. and M.Sc. degrees from Tianjin University, Tianjin, China, in 1993 and 1996, respectively, both in electrical engineering. She is currently working toward the Ph.D. degree at the National University of Singapore.

From 1996 to 2000, she was a Research Engineer with the Institute of Electronics, Chinese Academy of Sciences, Beijing, China. Her research interests include EMC/EMI modeling and simulation, parallel computing and signal integrity for high-speed electronic circuits and systems.

Wei-Liang Yuan (M'01) received the B.Sc., M.Sc., and Ph.D. degrees from Xidian University, Xi'an, China, in 1993, 1996, and 1999, respectively, all in electrical engineering.

Since 1999, he has been with the Institute of High Performance Computing, Singapore, where he is currently a Senior Research Engineer. His main research interests are in computational electromagnetics, electromagnetic compatibility, and signal integrity analysis.